JOURNAL OF MATERIALS SCIENCE **34** (1999) 6087–6093

Luminescence quenching in ZnS nanoparticles due to Fe and Ni doping

P. H. BORSE, N. DESHMUKH
Centre for Advanced studies in Materials Science and Solid State Physics, Department of Physics, University of Pune, Pune 411 007, India

R. F. SHINDE, S. K. DATE
National Chemical Laboratory, Pashan, Pune 411 008, India

S. K. KULKARNI
Centre for Advanced studies in Materials Science and Solid State Physics, Department of Physics, University of Pune, Pune 411 007, India
E-mail: skk@physics.unipune.ernet.in

Nanoparticles of zinc sulphide have been synthesized by a chemical method. Mercaptoethanol is used to passivate the surface of the particles. Under certain conditions highly luminescent particles emitting blue light at ~425 nm can be synthesized. This blue light emission in nanoparticles of zinc sulphide is observed to be completely quenched when doped with iron or nickel metal ions.

1. Introduction

Semiconductor nanoparticles has been a topic of great interest ever since [1–4] quantum confinement effect of photogenerated electrons and holes was experimentally observed as well as theoretically justified. One of the most striking observation due to quantum confinement effect is the 'blue shift' in optical absorption spectra and enhancement of excitonic peak with reduction in particle size. The particle size below which the blue shift occurs is often termed as 'critical size' which is the Bohr radius of excitons in semiconductors. Bohr radius of exciton is extremely small in some of the semiconductors like zinc sulphide (~1.1 nm). Synthesis and characterization of semiconductor nanoparticles with a narrow size distribution is therefore quite a challenging job. A number of structured media have been used [5–9] like glasses, zeolites, polymers etc. to obtain semiconductor nanoparticles in a narrow size range. Such nanoparticle embedded media or 'nanocomposites' are useful for a variety of applications and have been recently reviewed by Beecroft and Ober [10].

We have adopted a chemical route of semiconductor nanoparticles synthesis in which an organic capping agent is added to the reacting solutions during the synthesis. In this communication we present some of our results on doped and undoped zinc sulphide nanoparticles. Zinc sulphide semiconductor is widely used as a phosphor material. It is doped with a variety of transition metal ions to obtain the emission in different spectral regions. It is however interesting to use nanoparticles of ZnS in place of conventional bulk powder material. Due to spatial confinement of photogenerated electron-hole pairs they may behave differently in nanoparticles. This was particularly necessary in view of the photoluminescence of copper and manganese doped ZnS [11–13] and chromium doped Al_2O_3 [14] discussed in case of nanocrystallites as compared to bulk materials. We have reported earlier [11, 12] that copper and manganese can be successfully doped in zinc sulphide nanoparticles even at room temperature by the chemical method. Here we show the effect of iron and nickel metal ion doping on the quenching of blue light emitted by zinc sulphide nanoparticles.

2. Experimental

Synthesis of zinc sulphide nanoparticles has been carried out using a chemical method described in some earlier paper. Procedure in brief is as follows. Aqueous solutions of zinc, nickel and iron chlorides, sodium sulphide and mercaptoethanol were prepared. Synthesis of undoped zinc sulphide nanoparticles was made by mixing zinc chloride and mercaptoethanol under nitrogen atmosphere in a glass reactor. The solution was vigorously stirred for an hour. To this solution sodium sulphide was dropwise added. The resulting product viz. zinc sulphide nanoparticles capped with mercaptoethanol chains begin to precipitate when solution stirring is stopped. The precipitate is washed several times in water to remove unreacted sodium, zinc etc. By centrifuging and drying free standing powders of zinc sulphide nanoparticles which appear white in color are obtained. The powders are highly stable and do not show any coalescence or agglomeration even after several months. By changing the concentrations of zinc chloride, sodium sulphide and mercaptoethanol it is possible to obtain nanoparticles with different sizes, and of varying energy gap. This was shown earlier [15] in case of cadmium sulphide nanoparticles. In order to dope zinc sulphide nanoparticles with either nickel or

iron, aqueous solutions of $NiCl_2$ or $FeCl_3$ were added to a solution of zinc chloride and mercaptoethanol before reacting them with sodium sulphide. In the present case aqueous solution of 10^{-2} molarity of zinc chloride, nickel chloride, iron chloride, sodium sulphide and mercaptoethanol were prepared. For doping with various amounts 0.01, 0.10, 1.0 and 5.0% of nickel chloride and iron chloride (by volume) were added to 50% (by volume) of zinc chloride and sodium sulphide.

Analysis of nanoparticles was carried out using different techniques like optical absorption, photoluminescence, X-ray diffraction, atomic absorption, X-ray photoelectron spectroscopy and electron spin resonance. This is described below.

Optical absorption spectra were obtained using Shimadzu UV 300 double beam spectrophotometer. The spectral range used in this case was 200 to 500 nm. Samples used in this case were in the form of solutions prepared by dispersing the nanoparticle powders in distilled water. It was confirmed that neither mercaptoethanol nor other chemicals used in the synthesis produce any absorption feature in this range.

X-ray diffraction analysis of dry nanoparticle powders was made using Phillips PW 1840 powder X-ray diffractometer. CuK_α ($\lambda = 1.54$ A$^\circ$) was used as the source of X-rays. Diffraction patterns were recorded over a range of 15 to 70°.

In order to check the presence of any unexpected impurity photoelectron spectroscopy analysis of dry powders was carried out using a commercial model ESCALAB MK II of VG Scientific U.K. MgK_α ($h\nu = 1253.6$ eV) served as the source of radiation and photoelectrons were analyzed using a concentric hemispherical analyzer at a 50 eV pass energy. Au $4f_{7/2}$ at 84.0 ± 0.2 eV is used as the external and C1s at 285.0 ± 0.2 eV as the internal standard.

Further, photoluminescence work was carried out using Perkin Elmer LS-50 spectrometer. Here xenon lamp was used as a source of excitation and different excitation wavelengths or emission regions were chosen using appropriate filters. A spectral range of 200 to 900 nm could be chosen. Samples in the form of dry powders were used.

Electron spin resonance (ESR) investigations of iron doped ZnS samples were made using Brucker-ER-200-D X band spectrometer. For this all the samples of equal weight were taken and measurements were done at room temperature. A 100 kHz field modulation was used and the spectra were recorded in the absorption mode as the first derivative of the signal.

3. Results and discussion

There are many reports dealing with nanoparticles obtained by a variety of techniques. Chemical synthesis of nanoparticles in the form of colloidal solutions, free standing powders or particles embedded in some solid media like glass, polymers, zeolites etc. are well established techniques now. We have preferred to synthesize nanoparticles of zinc sulphide by chemical method for a variety of reasons. First of all it is rather simple and inexpensive method in which reaction is carried out at room temperature. The nanoparticles of zinc sulphide with particle size less than ~5 nm can be easily produced. Nanoparticles obtained here are probably bonded through sulphur end of the mercaptoethanol viz. sulphur in zinc sulphide. Mercaptoethanol covered particles of zinc sulphide do not coalesce to form bigger particles, even after an extensive period of time. Particles are suspended like colloids in solutions and can be easily subjected to optical absorption investigations. Besides as shown earlier the doping of the transition metal ions is also very easy. Thus unlike bulk ZnS doping carried out by thermal diffusion at high temperature it is possible to dope the nanoparticles at room temperature and doping in desired amount. It is possible to obtain particle size variation just by changing the molarity (M) of $ZnCl_2$ and Na_2S and keeping molarity of the mercaptoethanol constant. Fig. 1 gives the optical absorption spectra of ZnS nanoparticles. The bulk band gap of ZnS is 3.68 eV and absorption peak is expected at 337 nm. Here it can be seen that absorption peak has shifted even upto 270 nm corresponding to an energy gap of ~4.59 eV. This is a large change in the energy gap of ZnS nanoparticles. Although not shown here, one can also change molarity of capping agent viz. mercaptoethanol in this case to achieve the same effect. In Table I, the positions of excitonic peaks or energy gap variation with $ZnCl_2$ and Na_2S molarity are shown. Here mercaptoethanol molarity is kept constant. It can be seen that when molarity of the reactants reduces, smaller particles are obtained. Also the excitonic peaks become more prominent with reduction in the particle size. Kayanuma [16] has shown that such an enhancement in the intensity of an excitonic peak can be attributed to the increased oscillator strength of nanoparticles. Photoluminescence studies

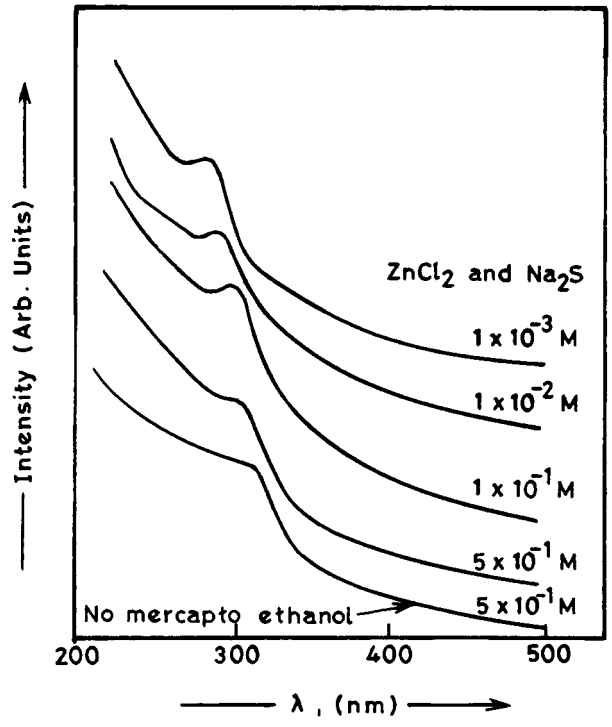

Figure 1 Optical absorption spectra of ZnS nanoparticles obtained by variation in molarity (M) of $ZnCl_2$ and Na_2S simultaneously from 5×10^{-1} to 1×10^{-3} M each keeping mercaptoethanol molarity constant (1×10^{-1} M).

TABLE I Energy gap of ZnS nanoparticles obtained by variation of concentration of $ZnCl_2$ and Na_2S keeping mercaptoethanol molarity constant at 10^{-1} M

$ZnCl_2$ and Na_2S Molarity (M)	Wavelength (nm)	Energy Gap (eV)
1×10^{-3}	270	4.59
1×10^{-2}	280	4.42
1×10^{-1}	290	4.20
5×10^{-1}	310	4.10
5×10^{-1}	320	3.87

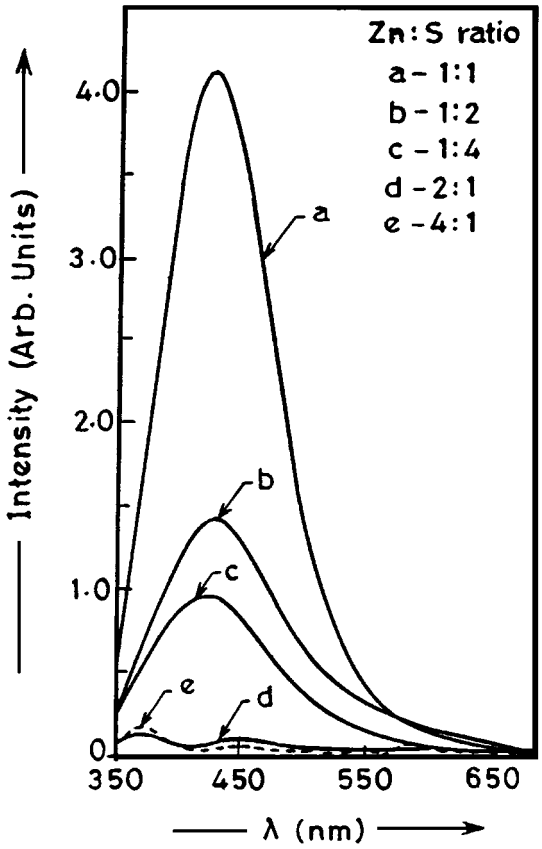

Figure 2 Photoluminescence spectra for varying Zn : S ratio.

of ZnS doped and undoped nanoparticles are interesting. In the colloidal solution these are widely investigated [3, 17] for their optical properties. There are a few reports on ZnS nanoparticles in solid media also [13, 18]. One observes a strong photoluminescence at ∼425 nm. Dunstan *et al*. [17] have observed additional peaks at 480–500 nm and 550–570 nm. The peak at ∼420 nm was attributed to $(SO_4)^{2-}$ species adsorbed at the surface. The peaks at 480–500 nm and 550–570 nm were assigned to zinc and sulphur at the colloidal particle surface respectively. We have observed a very strong luminescence peak at ∼425 nm which we attribute to (S^{2-}) anion vacancy. Further by changing Zn : S ratio we notice that there is no effect on optical absorption spectra but photoluminescence intensity changes dramatically as seen in Fig. 2. Thus we notice that under certain condition only strong photoluminescence is observable. Note that Zn : S ratio mentioned here are those taken while reacting the solutions. Actual ratio of Zn : S incorporated in the particles may be different. It is possible that anion vacancies produce defect state which are responsible for observed photoluminescence. Even in Zn : S taken in equal amounts in the solution, there can be some anion defects. There is however an optimum amount of defects concentration at which photoluminescence is maximum and is at ∼425 nm. As maximum photoluminescence intensity was observed by keeping Zn : S ratio as one, for doping experiments this ratio is preferred.

Zinc sulphide being a phosphor material bulk doped ZnS semiconductors have been widely investigated [19–23] experimentally as well as theoretically. Effect of a variety of metal ions incorporation like Mn, Cu, Al, Na, Ag, Fe, Ni has been investigated. Effect of doping Mn and Cu in nanocrystallites of ZnS has shown [11, 12, 24] interesting effects in recent years. Thus it was shown by Bhargava *et al*. that quantum efficiency as high as 18% can be achieved in case of ZnS nanoparticles doped with manganese. The high quantum efficiency was attributed not only to faster energy transfer to Mn^{2+} ion but also the changed rate of luminescence decay. The faster decay times in case of nanoparticles is a consequence of strong sp-d mixing due to localization of electron and hole on Mn^{2+}. It was therefore thought worthwhile to see further effect of iron and nickel doping in nanoparticles.

The nanoparticles of ZnS obtained by taking zinc to sulphur ratio as one forms the reference sample. It gives an absorption peak at ∼290 nm. Doping concentration being very small nickel or iron even upto 5% by volume, do not show any change in the absorption peak and are not therefore shown here. This is also true for X-ray diffraction patterns shown for undoped ZnS nanoparticles and doped nanoparticles. In Fig. 3 diffraction pattern shows three distinct peaks. This clearly indicates that the nanoparticles are crystalline in nature. However due to very small size of

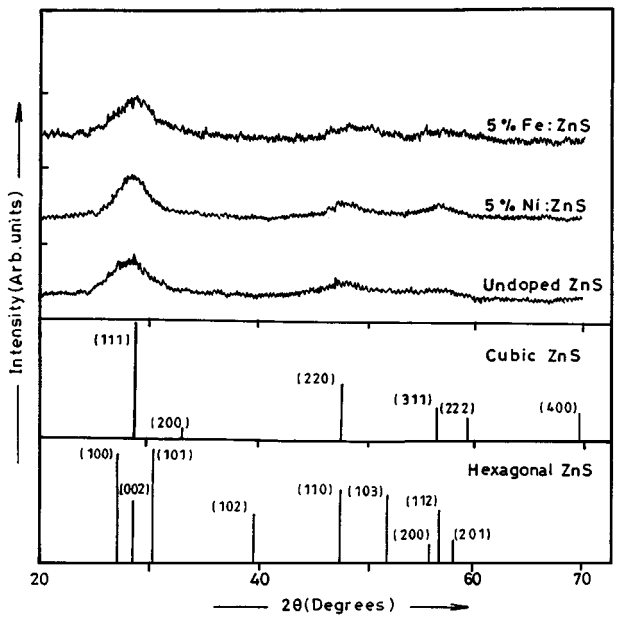

Figure 3 X-ray diffraction patterns for undoped and doped ZnS nanoparticles corresponding line spectra of bulk cubic and hexagonal structure of ZnS from standard JCPDS (Joint Committee on Powder Diffraction Standards) databases are also included.

nanoparticles under consideration, diffraction peaks have a substantial amount of width. Consequently (1 1 1) and (2 0 0) peaks of cubic ZnS appear as a single broad peak and so also (1 0 0) , (0 0 2) and (1 0 1) peaks of hexagonal phase. They also lie as shown in Fig. 3 at same angle. Similarly (2 2 0) peak of cubic ZnS and (1 1 0) peak of hexagonal ZnS lie at about same angle. Similarly hexagonal ZnS produces a single peak in place of (2 0 0), (1 1 2) and perhaps (2 0 1) plane. A diffraction peak due to (3 1 1) and (2 2 2) in cubic ZnS is also possible. In case of CdS Bandarnayke *et al*. [25] attributed a similar diffraction pattern of CdS to cubic structure as (1 0 2) and (1 0 3) peaks were absent. However Vogel *et al*. [26] have shown the possibility of presence of hexagonal phase. Scherrer formula has been used for particle size determination

$$d = \frac{0.94\,\lambda}{\beta \cos\,\theta} \qquad (1)$$

Where β is full width at half maxima (FWHM), θ is the angle of diffraction and λ is the wavelength of incident radiation, d is the size of particle. An average particle size has been estimated as $\sim 2.0 \pm 0.2$ nm.

Concentrations of doped metal ions viz. nickel and iron was determined using atomic absorption spectroscopy. Tables II and III give the concentration of iron and nickel taken by volume percentage and that actually obtained. We have monitored the effect of iron and nickel doping on the photoluminescence intensity at ~425 nm in undoped ZnS. In both the cases i.e. by doping iron or nickel we observed a dramatic effect on photoluminescence intensity. As shown in Fig. 4 for iron and Fig. 5 for nickel ions quenching of intensity is obvious. Insets of figures also show how the intensity drops with the increasing concentration of nickel and iron. It is known in bulk material [22, 23] that iron

TABLE II Concentration of iron doped in weight percentage in ZnS nanoparticle and concentration actually obtained

Sample	Concentration of Fe doped wt %	Concentration detected from AAS wt %
Undoped	0.00	0.008
0.1%	0.12	0.101
1.0%	1.20	0.758
5%	5.85	3.16

TABLE III Concentration of nickel doped in weight percentage in ZnS nanoparticle and concentration actually obtained

Sample	Concentration of Ni doped wt %	Concentration detected from AAS wt %
Undoped	0.00	0.010
0.01%	0.011	0.022
0.1%	0.111	0.030
1.0%	1.114	0.046
5%	5.57	0.099

and nickel are doped substitutionally in ZnS. They act as electron trapping centers which results into non-radiative recombination. This means that photo-excited electrons are preferentially transferred to nickel and iron metal ion induced trapping centers compared to anion vacancy defect centers. Quenching of photoluminescence peak at ~425 nm in ZnS colloidal particles by Cd^{2+} ions was investigated by Weller *et al*. [18]. They observed that addition of Cd^{2+} ions shifted the luminescence peak to 580 nm and the intensity of the peak kept on reducing with increased amount of Cd^{2+} ions concentration. They have attributed this behavior to the formation of co-colloids. It is speculated that Zn^{2+} ions are being replaced by Cd^{2+} ions at the surface of the particles. These are considered to be responsible for the fluorescence observed at 580 nm. However it is possible

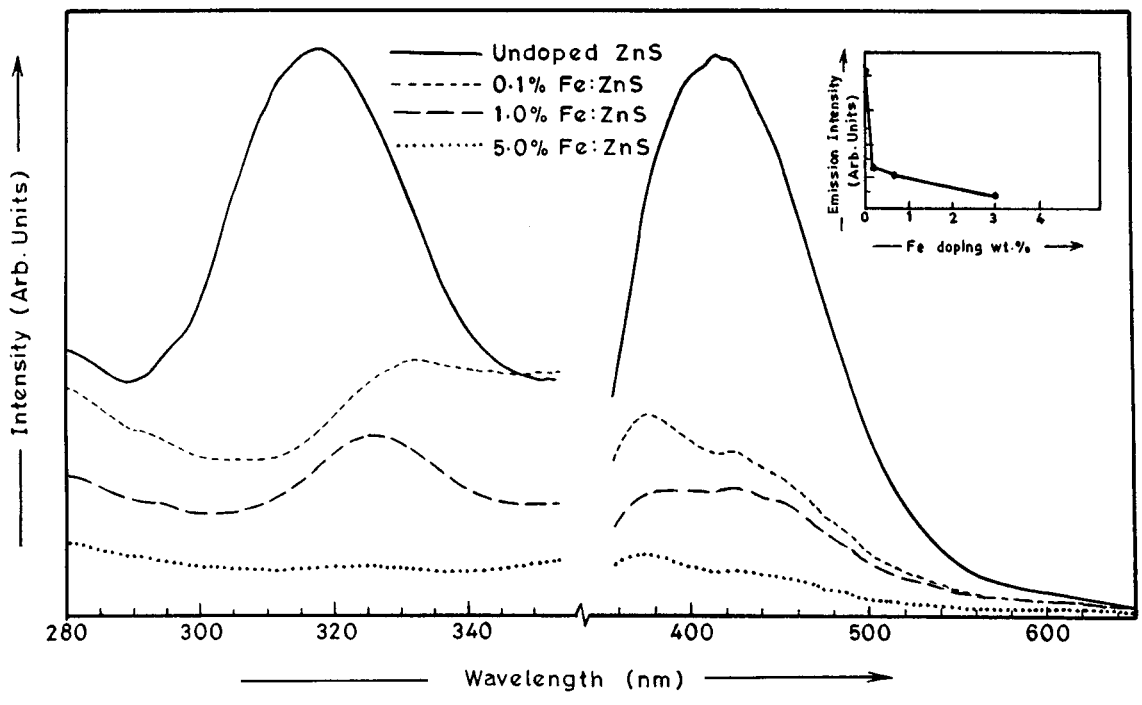

Figure 4 Excitation and emission spectra for undoped and iron doped ZnS nanoparticles.

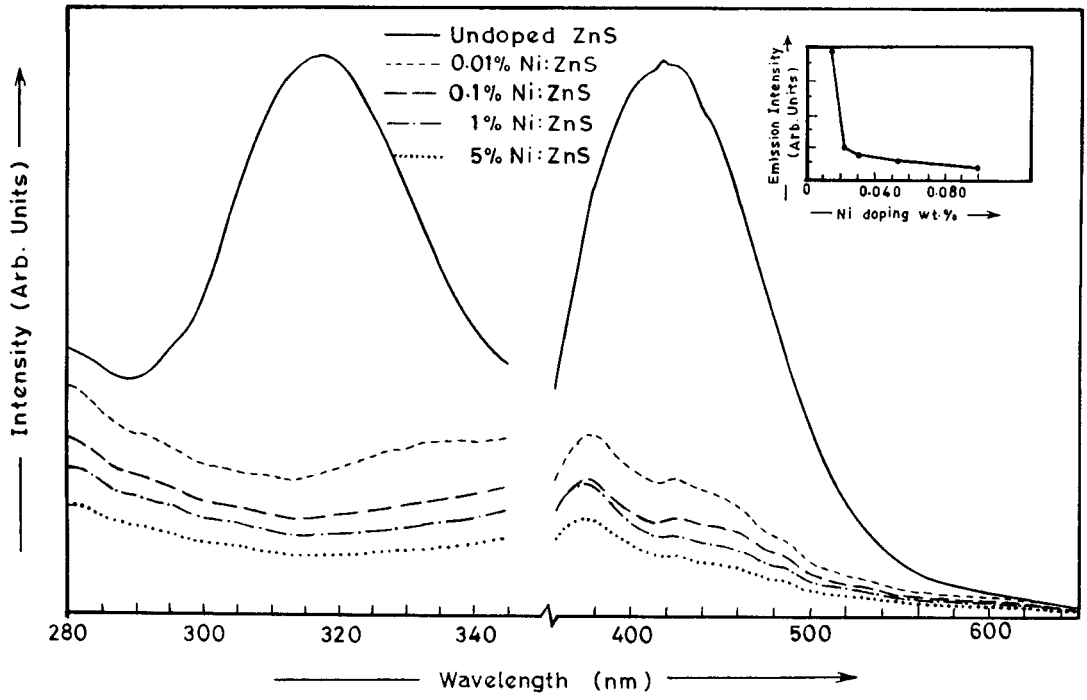

Figure 5 Excitation and emission spectra for undoped and nickel doped ZnS nanoparticles.

to quench the luminescence peak at 425 nm by doping of iron or nickel in ZnS network if there is more positive charge relative to the lattice.

In order to throw more light on the valency of doped ions we have carried out ESR of iron doped and undoped samples of ZnS. In Fig. 6, ESR spectra show absorption intensity of microwaves in nanoparticle sample with different doping level of iron against the applied field. Spectra are recorded in the derivative mode for ZnS nanoparticles used in the photoluminescence work shown in Figs 4 and 5. In case of ESR spectrum for undoped ZnS nanoparticle, it shows hyperfine splitting due to manganese. Hence $g \sim 2$ for this characteristic feature is assigned to Mn^{2+} in ZnS. Similarly the ESR signal also gives $g \sim 2$ which is due to Fe^{3+}. However these intrinsic elements are not detected by atomic absorption studies, as the concentration of manganese was less than 10^{-3} wt % and did not have any effect on photoluminescence. Mn^{2+} shows characteristic luminescence at ∼592 nm which was absent in this case. Iron of course has an effect on photoluminescence quenching as seen above. Removal of even $<10^{-3}$ wt % of Fe may turnout to be advantageous to further increase the blue luminescence in ZnS. ESR at the same time proves here to be a valuable tool to detect the impurities at lower concentration, unlike atomic absorption. Doping of 0.1 % Fe gives higher ESR intensity (spin density), $g \sim 2.4$ which do not match with known states of Fe. Tentatively g value can be assigned to Fe^{+} ($g \sim 2.2$) and Fe^{3+} ($g \sim 2.0$) as assigned by Surma *et al.* [27]. The larger g value in this case is attributed to interaction of Fe ions with defect states there by making charge of lattice more positive resulting in quenching of blue luminescence. For higher concentration of 1% and 5% Fe, ESR intensity is reducing due to clustering of Fe ions, resulting in 'concentration quenching' of blue luminescence. Increasing amount of doped iron ions substantially modify the ESR spectra as evident from Fig. 6. There is considerable change in the peak width. This may be due to clustering. Thus clustering of Fe-Fe ions play active role in concentration quenching. This also can be noticed from the inset of Fig. 6, which shows PL intensity is a function of spin density [28] obtained from ESR for various Fe concentrations in ZnS nanoparticles.

Further we have carried out photoelectron spectroscopy of doped as well as undoped samples. Fig. 7 gives the survey scans for the samples. They reveal the existence of S, C, O, Zn elements in ZnS nanoparticles. No other detectable amount of impurity is present. We also did not observe any $(SO_4)^{2-}$ species. This indicates that oxidation of ZnS nanoparticles probably has not occurred. Even though samples of maximum doping (5%) of Ni and Fe are used for XPS analysis Ni and Fe are not detected. It is known from atomic absorption studies that these elements are present in nanoparticle with very low concentrations (see Table II and III). The presence of carbon and oxygen is obvious as mercaptoethanol (C_2H_5OSH) is used as capping agent. The Zn 2p XPS core level appeared at 1022.0 eV corresponds to ZnS [29]. The quantitative analysis of samples is rather difficult as sulphur is present in both in core of ZnS nanoparticle as sulphide and in mercaptoethanol. Semiquantitative analysis using standard atomic sensitivity factors [30] was performed and presented in Table IV.

TABLE IV Different ratios of elements as determined from XPS analysis

Sample	Zn/S ratio	Zn/C ratio
Undoped	0.2	0.2
5% Fe : ZnS	0.3	0.2
5% Ni : ZnS	0.3	0.2

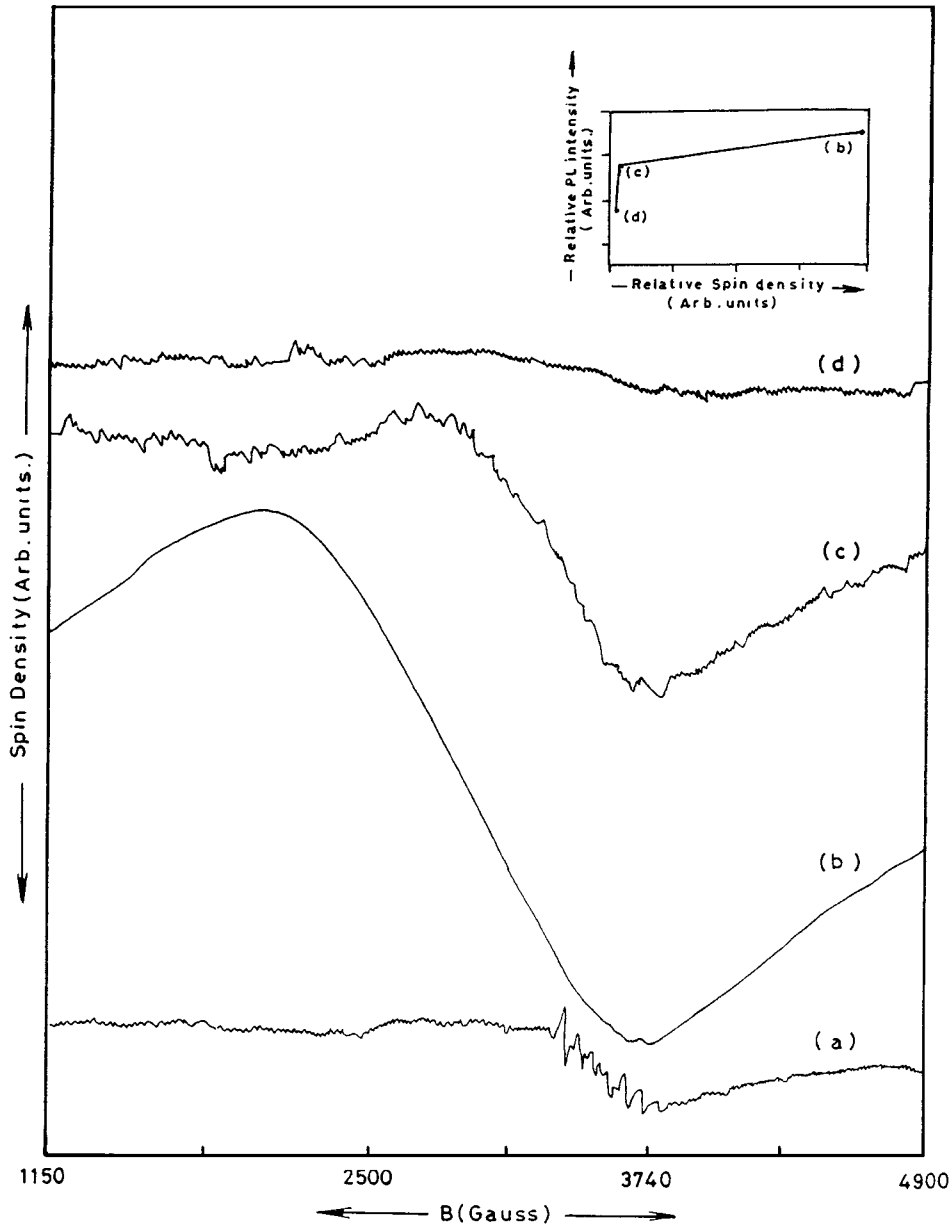

Figure 6 ESR spectra of undoped and iron doped ZnS nanoparticles with different concentrations (a) undoped, (b) 0.1% Fe : ZnS, (c) 1% Fe : ZnS and (d) 5% Fe : ZnS. Inset shows PL intensity as function of spin density, corresponding points of Fe concentration are marked, point (a) is excluded being for undoped.

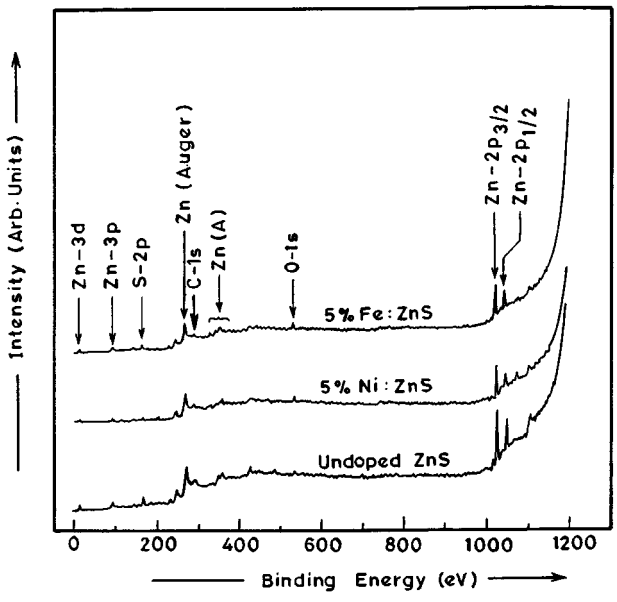

Figure 7 XPS survey scans of undoped and doped ZnS nanoparticles.

4. Conclusions

Zinc sulphide nanoparticles can produce intense blue emission at ~425 nm under certain conditions. This emission can be quenched by iron and nickel doping. In case of iron doping, iron ions are perhaps in the substitutional sites of Zn^{2+} Iron ions are observed to be in the Fe^{3+} state. Progressively increased doping of Fe^{3+} ions completely removes the emission peak at ~425 nm. Doping in ZnS smaller than $\sim 10^{-3}$ wt% were detected by ESR.

Acknowledgements

PB and ND would like to thank ISRO, India for fellowships. SKK would also like to thank Department of Science and Technology, Government of India for financial support. SKK would like to thank UGC, India for a continuous support.

References

1. AL. L. EFROS and AL. EFROS, *Sov. Phys. Semicond.* **16** (1982) 772.

2. L. E. BRUS, *Acc. Chem. Res*. **23** (1990) 183; *J. Phys. Chem*. **90** (1986) 2555; *J. Chem. Phys*. **80** (1984) 4403.
3. A. HENGLIEN, *Topics in current Chemistry* **143** (1988) 113; *Chem. Rev*. **89** (1989) 1861.
4. H. WELLER, *Angew. Chem*. **32** (1993) 42.
5. V. PTATSCHEK, B. SCHREDER and L. SPANHEL, *J. Phys. Chem. B* **101** (1997) 8898.
6. A. LIPOVSKII, E. KOLOBKAVA, V. PETRIKOV, I. KANG, A. OLKKOVETS, T. KRAUSS, M. THOMAS, J. SILCOX, F. WISE, Q. SHEN and S. KYCIA, *Appl. Phys. Lett*. **71** (1997) 3406.
7. G. D. STUCKY and J. E. MACDOUGALL, *Science* **247** (1990) 669.
8. Y. WANG and N. HERRON, *Chem. Phys. Lett*. **200** (1992) 71.
9. R. PREMACHANDRAN, S. BANERJEE and D. L. KAPLAN, *Chem. of Mater*. **9** (1997) 1342.
10. L. L BEECROFT and C. K. OBER, *Chem. Mater*. **9** (1997) 1302.
11. A. A. KHOSRAVI, M. KUNDU, L. JATWA, S. K. DESHPANDE, U. A. BHAGWAT, M. SASTRI and S. K. KULKARNI, *Appl. Phys. Lett*. **67** (1995) 2702.
12. A. A. KHOSRAVI, M. KUNDU, B. A. KURUVILLA, G. S. SHEKHAWAT, R. P. GUPTA, A. K. SHARMA, P. D. VYAS and S. K. KULKARNI, *ibid*. **67** (1995) 2506.
13. Q. CHEN, X. LI, Y. QIAN, J. ZHU, G. ZHOU, W. ZHANG and Y. ZHANG, *ibid*. **68** (1996) 3582.
14. P. BOROOJERDIAN, M. VEDPATHAK, M. KUNDU, V. D. GOGTE and S. K. KULKARNI, *High Temp. and Mat. Sci*. **36** (1996) 65.
15. M. KUNDU, A. A. KHOSRAVI and S. K. KULKARNI, *J. Mater. Sci*. **32** (1997) 245.
16. Y. KAYANUMA, *Phys. Rev. B* **38** (1988) 9777.
17. D. E. DUNSTAN, A. HAGFELDT, M. ALMGREN, H. O. G. SIEGBAHN and E. MUKHTAR, *J. Phys. Chem*. **94** (1990) 6797.
18. H. WELLER, U. KOCH, M. GUTIERREZ and A. HENGLIEN, *Ber. Bunsenges. Phys. Chem*. **88** (1984) 649.
19. H.-J. SCHULZ, *J. Cryst. Growth* **59** (1982) 65.
20. R. RENZ and H.-J. SCHULZ, *J. Phys. C* **16** (1983) 4917.
21. Z. TIAN and X. SHEN, *J. Appl. Phys*. **66** (1989) 2414.
22. P. M. JAFFE and E. BANKS, *J. Electrochem. Soc*. **111** (1964) 52.
23. H. A. WEAKLIEM, *J. Chem. Phys*. **36** (1962) 2117.
24. R. N. BHARGAVA, D. GALLAGHER, X. HONG and A. NURMIKKO, *Phys. Rev. Lett*. **72** (1994) 416.
25. R. J. BANDARANAYASKE, G. W. WEN, J. Y. LIN, H. X. JIANG and C. M. SORENSEN, *Appl. Phys. Lett*. **67** (1995) 831.
26. W. VOGEL, J. URBAN, M. KUNDU and S. K. KULKARNI, *Langmuir* **13** (1997) 827.
27. M. SURMA, A. J. ZAKRZEWSKI and M. GODLEWSKI, *Phys. Rev. B* **52** (1995) 11879.
28. C. P. POOLE, "Electron Spin Resonance- A Comprehensive Treatise on Experimental Techniques" (John Wiley & Sons, 1967) p. 800.
29. B. R. STROHMEIER and D. M. HERCULES, *J. Catalysis* **86** (1984) 266.
30. C. D. WAGNER, W. M. RIGGS, L. E. DAVIS, J. F. MOULDER and G. E. MUILENBERG, "Handbook of X-ray Photoelectron Spectroscppy" (Perkin-Elmer Corporation Minnesota, 1978).

Received 24 July 1998
and accepted 21 June 1999